HHS Public Access

Author manuscript

Hepatology. Author manuscript; available in PMC 2022 February 01.

Published in final edited form as:

Hepatology. 2021 February ; 73(2): 571–585. doi:10.1002/hep.31256.

Circulating extracellular vesicles carrying sphingolipid cargo for the diagnosis and dynamic risk profiling of alcoholic hepatitis

Tejasav S. Sehrawat, MBBS[1], **Juan P. Arab, MD**[1,2], **Mengfei Liu, MD**[1], **Pouya Amrollahi, MS**[3,4], **Meihua Wan, PhD**[3,4,5], **Jia Fan, PhD**[3,4], **Yasuhiko Nakao, MD**[1,6], **Elisa Pose, MD**[7,8,9], **Amaia Navarro-Corcuera, PhD**[1], **Debanjali Dasgupta, PhD**[1], **Chieh-Yu Liao, BS**[1], **Li He, MD**[1,10], **Amy S. Mauer, BS**[1], **Emma Avitabile, MD**[8], **Meritxell Ventura-Cots, MD**[11], **Ramon A. Bataller, MD**[11], **Arun J. Sanyal, MD**[12], **Naga P. Chalasani, MD**[13], **Julie K. Heimbach, MD**[14], **Kymberly D. Watt, MD**[1], **Gregory J. Gores, MD**[1], **Pere Gines, MD**[7,8,9], **Patrick S. Kamath, MD**[1], **Douglas A. Simonetto, MD**[1], **Tony Y. Hu, PhD**[3,4], **Vijay H. Shah, MD**[1,*], **Harmeet Malhi, MBBS**[1,*]

[1]Division of Gastroenterology and Hepatology, Mayo Clinic, MN, USA

[2]Departamento de Gastroenterologia, Escuela de Medicina, Pontificia Universidad Catolica de Chile, Santiago, Chile

[3]Virginia G. Piper Biodesign Center for Personalized Diagnostics, The Biodesign Institute, Arizona State University, Tempe, AZ, USA

[4]School of Biological and Health Systems Engineering, Arizona State University, Tempe, AZ, USA

[5]Department of Integrated Traditional Chinese and Western Medicine, West China Hospital of Sichuan University, Chengdu, Sichuan Province, China

[6]Nagasaki University Hospital, Nagasaki, Japan

[7]Liver Unit, Hospital Clinic De Barcelona, School of Medicine and Health Sciences, University of Barcelona, Barcelona, Spain

[8]Institut D'investigacions Biomediques August Pi I Sunyer (IDIBAPS), Barcelona, Spain

[9]Centro de Investigacion Biomedica en Red de Enfermedades Hepaticas y Digestivas (CIBEReHD), Barcelona, Spain

[*] Corresponding Authors: Vijay H. Shah, M.D. and Harmeet Malhi, M.B.B.S., Division of Gastroenterology and Hepatology, Mayo Clinic, 200 First Street SW | Rochester, MN 55905 | USA, Fax: +1-507-255-6318 | Phone: +1-507-255-6028, shah.vijay@mayo.edu, malhi.harmeet@mayo.edu.

Author Contributions:

T.S.S. contributed to study concept and design; acquisition, analysis and interpretation of data; statistical analysis; writing the first draft and finalizing the manuscript; and preparing figures. J.P.A contributed to acquisition and interpretation of data. M.L. contributed to interpretation of data, critical revision of manuscript, and statistical analysis. A.N.C. contributed to data acquisition and critical revision of manuscript. P.A., M.W., J.F., C.Y.L., L.H., and D.D. contributed to data acquisition. E.P., E.A., M.V.C., R.A.B., J.K.H., K.D.W., and P.G. contributed to biospecimen acquisition. A.J.S. and N.P.C. contributed to sample acquisition and critical revision of manuscript. R.A.B., P.G., G.J.G., and P.S.K. contributed to critical revision of manuscript and for important intellectual content throughout the study. D.A.S. contributed to study concept and design; interpretation of data; important intellectual content throughout the study; and critical revision of manuscript. T.Y.H. contributed to data acquisition and interpretation. V.H.S. and H.M. contributed to study concept, design, funding, and supervision; interpretation of data; critical revision of manuscript; important intellectual content throughout the study; and finalizing the manuscript. All authors read and approved the manuscript before submission.

[10]Division of Gastroenterology, Tongji Hospital, Tongji Medical College, Huazhong University of Science and Technology, Hubei Province, China

[11]Division of Gastroenterology, Hepatology and Nutrition, University of Pittsburgh Medical Center, PA, USA

[12]Division of Gastroenterology, Hepatology and Nutrition, Virginia Commonwealth University, VA, USA

[13]Division of Gastroenterology and Hepatology, Indiana University, IN, USA

[14]Division of Transplant Surgery, Mayo Clinic, MN, USA

Abstract

Background & Aims—Alcoholic hepatitis (AH) is diagnosed by clinical criteria, although several objective scores facilitate risk stratification. Extracellular vesicles (EVs) have emerged as novel biomarkers for many diseases and are also implicated in the pathogenesis of AH. Therefore, we investigated whether plasma EV concentration and sphingolipid cargo could serve as diagnostic biomarkers for AH and inform prognosis to permit dynamic risk profiling of AH subjects.

Approach & Results—EVs were isolated and quantified from plasma samples from healthy controls, heavy drinkers, and subjects with end-stage liver disease (ESLD) due to cholestatic liver diseases and non-alcoholic steatohepatitis, decompensated alcoholic cirrhosis (AC) and AH. Sphingolipids were quantified by tandem mass spectroscopy. The median plasma EV concentration was significantly higher in AH subjects (5.8×10^{11}/ml) compared to healthy controls (4.38×10^{10}/ml, $p<0.0001$), heavy drinkers (1.28×10^{11}/ml, $p<0.0001$), and ESLD (5.35×10^{10}/ml, $p<0.0001$) and decompensated AC (9.2×10^{10}/ml, $p<0.0001$) disease controls. Among AH subjects, EV concentration correlated with MELD score. When EV counts were dichotomized at the median, survival probability for AH subjects at 90 days was 63.0% in the high EV group and 90.0% in the low EV group (logrank p-value=0.015). Interestingly, EV sphingolipid cargo was significantly enriched in AH when compared with healthy controls, heavy drinkers, ESLD and decompensated AC (p=0.0001). Multiple sphingolipids demonstrated good diagnostic and prognostic performance as biomarkers for AH.

Conclusions—Circulating EV concentration and sphingolipid cargo signature can be used in the diagnosis and differentiation of AH from heavy drinkers, decompensated alcoholic cirrhosis, and other etiologies of end-stage liver disease and predict 90-day survival permitting dynamic risk profiling.

Keywords

Exosomes; microvesicles; ceramide; prognosis; STOPAH; alcoholic liver disease; alcohol-associated liver disease; biomarker; biopsy

INTRODUCTION

Alcohol-associated liver disease (ALD) has been recognized as the most common cause of advanced liver disease worldwide and accounts for 50% of deaths due to cirrhosis (1–3).

ALD encompasses a wide spectrum of liver disease ranging from reversible steatosis to steatohepatitis and cirrhosis (4, 5). Alcoholic hepatitis (AH) is the most severe form of ALD with an extensive inflammatory response and a 30-day mortality rate of 20–40% (6). The diagnosis of ALD remains predominantly clinico-pathological with liver biopsies performed in some cases (7, 8). Widespread use of liver biopsies is limited due to a risk of complications in hemodynamically unstable patients with severe coagulopathy (9). It is also impractical to follow-up response to treatment with serial liver biopsies. Clinical decision-making is aided by static and dynamic scores such as the Model for End Stage Liver Disease (MELD), Maddrey's Discriminant Function (MDF), Lille score, and others, which are used to determine mortality, disease severity, and therapeutic response (9–12). These scores utilize readily available biochemical variables such as bilirubin, prothrombin time, creatinine etc. but are not disease-specific. Owing to the limitations of these tests, there is an unmet need to utilize new technology to identify novel, reproducible, efficient, and non-invasive biomarkers, especially those that are coupled with an advanced understanding of disease pathophysiology (5).

In recent years, extracellular vesicle (EV)-based biomarker discovery has gathered significant traction (13–15). EVs are nanometer-sized particles released by cells into their micro-environment and eventually enter circulation. Given their stability, presence in most biofluids, and signature cargoes, including sphingolipids, EVs have the potential to serve as circulating biomarkers (16). EVs are heterogeneous and are comprised primarily of exosomes and microvesicles. Operationally, the distinction between exosomes and microvesicles is less important as circulating vesicles are isolated according to their biophysical properties and consist of both types of EVs. Therefore, we have used the term EV throughout this manuscript, which is also in keeping with current society guidelines (13, 17, 18). EV numbers and cargo vary in disease. Previous studies have explored microRNAs and proteomic EV cargoes in preclinical models of AH (19). Sphingolipids, including ceramides, are implicated in inflammation, stress response, and apoptosis (20). Sphingolipids are also mechanistically crucial in EV formation (21, 22). Furthermore, sphingolipids have been implicated in AH pathogenesis (23–26). Thus, we evaluated EV count and sphingolipid cargo as a pathophysiologically relevant biomarker in AH.

In this paper, we show that EV counts can accurately diagnose AH by differentiating it from healthy controls; heavy drinkers; MELD matched end-stage liver disease (ESLD) due to non-alcoholic steatohepatitis (NASH), primary biliary cholangitis (PBC), primary sclerosing cholangitis (PSC), and biopsy proven decompensated alcoholic cirrhosis (AC) without acute AH. Furthermore, we explored the potentially additive role of EV counts and sphingolipid cargo to MELD and show that this proposed additive score (E-MELD) can predict disease severity and mortality.

METHODS

Sample Collection and Study Design

Blood samples from 36 heavy drinkers and 36 AH subjects were prospectively collected as a part of National Institute of Alcoholism and Alcohol Abuse (NIAAA) Translational Research and Evolving Alcoholic Hepatitis Treatment (TREAT) consortium 001 study at

Mayo Clinic (Minnesota, USA), Virginia Commonwealth University (Virginia, USA), and Indiana University (Indiana, USA). The consortium design has previously been reported (27). Samples from 7 additional AH subjects were obtained from University of Pittsburgh (Philadelphia, USA). We also obtained samples from 22 subjects with biopsy proven AH and 30 subjects with decompensated AC, biopsy proven to be negative for AH, from Hospital Clinic De Barcelona (Barcelona, Spain). Twenty-nine additional subjects with severe end-stage liver disease (MELD score>20) due to etiologies other than ALD, including NASH, PSC, and PBC, were prospectively recruited at Mayo Clinic and included as controls for MELD score > 20 group. Thirty-six healthy control samples from Mayo Clinic P30 biorepository were also included in the analysis. Eighteen AH subjects and 18 healthy controls from TREAT consortium were randomly included in the discovery cohort, and the remaining 25 AH subjects and 18 healthy controls from TREAT consortium and UPMC were included in the validation cohort.

The diagnosis of heavy drinkers and AH was confirmed in the clinical setting by an experienced hepatologist using NIAAA criteria as described here (28, 29). Heavy alcohol drinking was defined as consumption of > 40 grams of alcohol per day on average in women and > 60 grams of alcohol per day on average in men for a minimum of 6 months and within 6 weeks prior to study enrollment. Criteria for inclusion in the heavy drinker group included: (i) Aspartate Aminotranferase (AST), Alanine Aminotranferase (ALT), and total bilirubin levels within normal range; (ii) no prior history of known ALD; and (iii) absence of hepatosplenomegaly (from physical examination or radiographic imaging) or stigmata of liver disease. The diagnosis of AH was established following published criteria based on history of heavy alcohol consumption, clinical evaluation and appropriate laboratory testing (as defined as total bilirubin > 2 mg/dL, ALT and AST > 50 U/L but ≤500 U/L, and AST/ALT of ≥1.5). When a diagnosis of AH remained in question, a liver biopsy was pursued (28, 29). Blood was collected in ethylenediaminetetraacetic acid tubes, and platelet-poor plasma was separated. Plasma aliquots were stored at −80°C. EV isolation and analyses were performed in a blinded manner using ultracentrifugation technique (30–34). Details are provided in Supplemental Material. Plasma aliquots were thawed only once, immediately before EV isolation. The study was approved by a central institutional review board as well as individual institutional review boards at all involved sites. The study protocol conformed to the ethical guidelines of the 1975 Declaration of Helsinki as reflected in *a priori* approval by the appropriate institutional review committee. All samples were collected after written informed consent was obtained from each subject. All authors had access to the study data and reviewed and approved the final manuscript.

Targeted Sphingolipid Measurement of Plasma and EV Fractions

Concentrations of sphingolipids were measured by liquid chromatograph/mass spectrometry (LC/MS/MS) by Mayo Metabolomics Core which is an NIH Regional Comprehensive Metabolomics Resource Core. The Core has developed and deposited detailed standard operating procedures for sphingolipid measurements to the Metabolomics Workbench (https://www.metabolomicsworkbench.org), a resource sponsored by the Common Fund of the National Institutes of Health. Details are provided in Supplemental Material.

Statistical Analyses

Subjects were characterized into MELD score groups of ≤20 and >20 based on current consensus guidelines (9, 29, 35). Continuous variables were summarized as mean or median and standard error as appropriate. Sample comparisons between groups using the Mann-Whitney U test, one-way ANOVA, or two-way ANOVA were performed as appropriate with post-test corrections when needed. The diagnostic accuracy parameters and associations were estimated using receiver operating characteristic (ROC) curve analysis. Area under the ROC curves (AUROC) with corresponding 95% confidence intervals (CI) and p values were calculated. Youden's index was used to establish a diagnostic cut-off in the discovery cohort where sensitivity and specificity reached maximum value with convergence. Kaplan-Meier (KM) survival curves were plotted to estimate the cumulative survival probability. The significance of observed differences and hazard ratios were calculated using logrank tests. The association between sphingolipids and clinical outcomes was determined using univariate Cox regression models. For statistical analyses and graphical and tabular preparations, GraphPad Prism 8 (GraphPad Software Inc, La Jolla, CA) and R-studio (https://cran.r-project.org) were used. R-packages pROC (for ROC curves); cutpointr (for Youden's index calculations); ggplot2 (for PCA plots); complexheatmap (for heatmap) and survival (for Kaplan-Meier curve analysis) were used.

RESULTS

Characterization of Subjects and EVs

Subjects included healthy controls, heavy drinkers, ESLD with MELD score >20, decompensated AC, and AH. Subjects with AH were divided into mild/moderate or severe based on recommended MELD score cut-off of 20 (28). Subject characteristics are described in Supplemental Table 1. The concentration of EVs isolated from plasma ranged between 2.8×10^9 and 2.5×10^{12} EVs/ml in all subjects [Table 1]. The median concentration of EVs in healthy controls, heavy drinkers, ESLD, decompensated AC, and AH subjects was 4.38×10^{10}, 1.28×10^{11}, 3.06×10^{10}, 6.29×10^{10}, 9.2×10^{10}, and 5.38×10^{11} particles/ml respectively [Table 1]. Plasma EV concentrations were significantly higher among AH subjects than healthy controls ($p<0.0001$), heavy drinkers ($p=0.0001$), ESLD subjects ($p<0.0001$), and decompensated AC ($p<0.0001$) [Figures 1A–B]. Moreover, the median EV counts were significantly higher in subjects with severe AH when compared with mild/moderate AH subjects ($p=0.0041$) [Figure 1C]. EV counts correlated well with traditional clinical risk stratifiers, such as the MELD and CTP scores [Figure 1D]. Interestingly, plasma EV concentrations were also significantly higher in heavy drinkers (median= 1.28×10^{11} EVs/ml) when compared with healthy controls (median= 4.38×10^{10}; $p=0.003$). The mean sizes of isolated EVs were 124.3 (healthy controls), 136.6 (heavy drinkers), 126.3 (ESLD), 131 (decompensated AC), and 127.4 (AH) nm and all within small EV size range of 50–150 nm [Supplemental Figure 1A]. The isolated and enriched small EVs expressed EV-specific protein markers cluster of differentiation 81 (CD81; transmembrane protein) and tumor susceptibility gene 101 (TSG101; cytosolic protein recovered in EVs) [Supplementary Figure 1B]. Thus, EV counts are significantly higher in AH subjects when compared to ESLD and decompensated AC subjects.

Threshold Detection and Validation of Extracellular Vesicle Count for the Diagnosis of Alcoholic Hepatitis

With the aim of establishing a diagnostic threshold, we randomly divided healthy controls and AH subjects from the TREAT consortium in half to establish a discovery cohort. First an ROC curve was generated for the diagnosis of AH vs. healthy controls and the AUROC curve value was 0.99 (95% CI 0.97 to 1.00; p<0.0001) [Figure 2A and Supplemental Figure 2A]. A threshold of 1.56×10^{11} EVs/ml was determined using Youden's index to differentiate AH subjects from healthy controls with a sensitivity of 1.00 (95% CI 0.81 to 1.00) and a specificity of 0.89 (95% CI 0.65 to 0.99). The performance of this diagnostic threshold to diagnose AH was tested in a validation cohort. The validation cohort consisted of 25 AH subjects and 18 healthy controls from TREAT consortium and UPMC. This diagnostic threshold of 1.56×10^{11} EVs/ml yielded a significantly (p<0.0001) high sensitivity of 0.92 (95% CI 0.75, 0.99) and specificity of 0.94 (95 % CI 0.74, 1.00) for distinguishing subjects with AH from healthy controls [Supplemental Figure 2B and Supplemental Table 2].

We next sought to test the ability of this diagnostic threshold to differentiate AH from heavy drinkers and disease controls with ESLD and decompensated AC. All of these analyses were performed in complete subject cohorts. This diagnostic threshold was able to differentiate AH subjects from heavy drinkers with a sensitivity of 0.93 (95% CI 0.84, 0.98) and a specificity of 0.73 (95% CI 0.54, 0.88) and an AUROC curve of 0.92 (95% CI 0.87, 0.98; p<0.0001) [Supplemental Table 2 and Supplemental Figures 2C–D]. Furthermore, this diagnostic threshold was able to differentiate AH from ESLD subjects with a sensitivity of 0.95 (95% CI 0.84 to 0.99) and specificity of 0.90 (95% CI 0.73 to 0.98), and an AUROC curve of 0.99 (95% CI 0.97, 1.00; p<0.0001) [Figures 2B–C and Supplemental Figure 2]. Similarly, it was able to differentiate AH from decompensated AC with a sensitivity of 0.94 (95% CI 0.85 to 0.98) and a specificity of 0.77 (95% CI 0.58 to 0.90) based on ROC curve (AUROC: 0.88; p<0.0001) analysis [Figure 2D and Supplemental Figure 2]. This initial analysis confirmed that EVs are significantly elevated in AH and could be of clinical utility. Thus the EV concentration diagnostic threshold of 1.56×10^{11} EVs/ml can diagnose AH from subjects with ESLD and decompensated AC.

Detecting Hepatocyte-Derived EVs in AH subjects

In order to demonstrate an increase in hepatocyte-derived EVs and translate an EV-based biomarker to a potential point-of-care test, we utilized a novel far-field nano-plasmonic enhanced scattering nPES assay (36). This technique can quantify cell-specific EVs directly from 1–5 pL plasma thus obviating the need for EV isolation. We identified cytochrome P450 2E1 (CYP2E1) and asialoglycoprotein receptor 2 (ASGR2) as two hepatocyte specific markers present on EV surface and utilized these to quantify EVs of hepatocyte origin and identifying differences between AH, healthy controls, and heavy drinkers (37, 38). The ASGR2 signal was significantly higher in AH when compared with healthy controls (p<0.0001) and heavy drinkers (p=0.04) [Figure 3A]. The CYP2E1 signal was significantly higher in AH when compared with healthy controls (p<0.0001) and heavy drinkers (p=0.009) as well [Figure 3B]. In keeping with the nPES data, the expression of hepatocyte-specific markers ASGR2 and CYP2E1 was determined to be higher in AH subjects

compared with controls by western-blotting [Figure 3C] and dual-immunogold transmission electron microscopy [Figure 3D]. Thus, there is an increase in hepatocyte-derived EVs in subjects with AH in comparison to healthy controls and heavy drinkers.

Predicting Survival with EV Concentration in AH subjects

After establishing a diagnostic threshold for AH, we sought to investigate the association between EV counts and 90-day survival in AH. Ninety-day survival follow-up data was available in 57 AH subjects. In order to study this association, we dichotomized these AH subjects into arbitrary low and high EV count groups using median EV count in our cohort (5.38×10^{11} EVs/ml) [Figure 4A]. There were a total of 13 deaths reported at 90-day follow up. Of note, 10 deaths were reported in the high EV group vs. 3 deaths in the low EV group. On KM analysis, the mortality risk in subjects with AH at 90-day follow-up was 37.0% in the high EV group and 10% in the low EV group (logrank test p=0.015 and logrank hazard ratio=4.3, 95% CI 1.5 to 13.0) [Figure 4B]. Thus, an EV concentration higher than 5.38×10^{11} EVs/ml predicts a much higher mortality risk in subjects with AH.

EV Cargo and Plasma Sphingolipids Concentration Analysis

Taking into account the aforementioned biologic relevance of EV cargo and role of bioactive sphingolipids in alcohol-induced injury, we performed targeted sphingolipid measurements on isolated EVs and plasma samples from healthy controls, heavy drinkers, ESLD, decompensated AC, and AH subjects. Eleven sphingolipid species were detected from plasma and EV cargo in varying concentrations. These included sphingosine, sphinganine, sphingosine 1-phosphate, C14:0 ceramide, C16:0 ceramide, C18:0 ceramide, C18:1 ceramide, C20:0 ceramide, C22:0 ceramide, C24:0 ceramide, and C24:1 ceramide. The analysis revealed significant differences in sphingolipid cargo content in EVs isolated from AH subjects when compared with healthy controls, heavy drinkers, ESLD, and decompensated AC subjects as evident by the heatmap and principle component analysis [Figure 5A–C]. Absolute concentrations of all sphingolipid species detected are provided in Supplemental Table 3 and Supplemental Figure 5. Of the 11 sphingolipids detected in the EVs, 6 were determined to have statistically-significant enrichment in AH subjects when compared with healthy controls, heavy drinkers, ESLD, and decompensated AC subjects [Figure 5D]. These included C14:0 ceramide, C16:0 ceramide, C18:0 ceramide, C20:0 ceramide, and C24:1 ceramide. Ten sphingolipid species were significantly enriched in AH when compared to healthy controls alone. This sphingolipid signature was found to be unique to EVs and similar trends were not observed in paired plasma samples [Figure 5E]. As sphingolipids are also found on lipoproteins, we wanted to confirm that the increase in EV sphingolipids was not due to a contribution from lipoproteins. Therefore, we examined the high density lipoprotein (HDL)-specific apoprotein, APOAI, and very low density lipoprotein (VLDL)/low density lipoprotein (LDL)-specific apoprotein, ApoB100, and found comparable expression across controls and AH. Thus, the increase in sphingolipids in AH was not due to a co-isolation of HDL, LDL or VLDL lipoproteins [Supplemental Figure 1C]. EV cargo sphingolipid concentrations were found to correlate well with EV counts, whereas plasma sphingolipid concentrations showed no similar trend [Supplemental Table 4]. Thus, a unique, long-chain ceramide-enriched sphingolipid cargo signature was identified in EVs from AH subjects.

Correlation of Extracellular Vesicle Sphingolipids with MELD and CTP Scores

We then interrogated an association between specific sphingolipid species and disease severity and mortality. By linear regression, significant positive correlations were found between MELD and log EV counts (r^2=0.475, p<0.0001) as well as all 11 detected EV cargo sphingolipids including sphingosine, sphinganine, sphingosine-1 phosphate, C14:0 ceramide, C16:0 ceramide, C18:0 ceramide, C18:1 ceramide, C20:0 ceramide, and C24:1 ceramide [Supplemental Table 5 and Supplemental Figure 3]. A similar significant positive correlation was also observed with CTP score and log EV count (r^2=0.441, p<0.0001) as well as all 11 detected EV count sphingolipids [Supplemental Table 6 and Supplemental Figure 4]. By linear regression, models against disease severity determined by both CTP and MELD scores, EV cargo sphingosine, sphinganine, sphingosine 1 phosphate, C14:0 ceramide, C16:0 ceramide, and C24:1 ceramide had significant positive correlations with r^2>0.3 and p<0.05. Thus, we found EV counts and sphingolipid cargo to correlate positively with MELD and CTP scores.

Performance of EV counts with EV Cargo Sphingolipids

We next adopted a combinatorial approach to determine if the interaction of EV sphingolipid content and EV count can predict mortality. Univariate Cox modeling was performed to ascertain risk association with 90-day mortality for each individual sphingolipid as well as EV × sphingolipid [Supplemental Table 7]. As expected, MELD score, CTP score, and total bilirubin were all associated with increased risk of mortality. In addition, 6 EV cargo sphingolipids sphingosine, sphinganine, sphingosine 1-phosphate, C14:0 ceramide, C16:0 ceramide, and C24:1 ceramide were predictive of higher mortality risk at 90-day follow up. When these significant risk factors for mortality were analyzed in a multivariate analysis, none attained statistical significance, likely due to limited sample size. The association of EVs and sphingolipids with disease severity (as determined by MELD and CTP scores) and mortality was then assessed and plotted in the form of ROC curves. Youden's index was used to determine optimal cutoffs for each individual sphingolipid when interacting with EV count as EV × sphingolipid [Figures 6–7 and Supplemental Tables 8–10]. Multiple sphingolipids had good discriminatory power in determining disease severity based on these cutoffs, but under-performed compared to the MELD score or EV count alone. KM curves were plotted for each potential biomarker based on these generated cutoffs, and their ability to prognosticate AH was determined [Figure 7 and Supplemental Table 9]. Performance of EV × Sphingolipid together had enhanced performance when considering disease severity or mortality as outcome [Figures 6–7]. Interestingly, the same 6 sphingolipids identified to have positive hazards ratios in the Cox's Univariate analysis were also found to prognosticate the mortality of AH subjects in KM curves with significance. An ROC curve was generated combining MELD score, log EV count and these 6 sphingolipid populations to generate an E-MELD score and determine association with 90-day mortality. The AUROC was determined to be 0.91. Thus, even though discriminatory capacity for MELD-logEV alone (AUC=0.86) was similar to MELD (AUC=0.86), E-MELD performed better (AUC=0.91) in predicting mortality [Figure 7B].

DISCUSSION

There is a significant unmet need for AH biomarkers that are specific, pathophysiologically-informed, amenable to repeated testing over time and predictive of both treatment response and clinical outcomes. Thus, the objective of this study was to demonstrate the utility of circulating EVs and their sphingolipid cargo as biomarkers for the diagnosis and prognosis of AH. The principal findings of this study include: i) EV cutoff of 1.56×10^{11} particles/ml can diagnose AH in comparison with heavy drinkers, healthy controls, decompensated alcoholic cirrhosis, and end-stage liver disease due to NASH or chronic cholestatic diseases; ii) AH EVs are significantly enriched in sphingolipid cargo, which is independently predictive of AH severity and mortality; and iii) incorporation of EV concentration and sphingolipid species (E-MELD) increase the performance of MELD score in predicting 90-day mortality (AUC=0.91 vs. 0.86).

The NIAAA and other expert consensus guidelines have defined the clinical criteria for diagnosis of AH with confirmation, if necessary, by histopathological examination (8, 28, 29). However, liver biopsy has risks and poor patient acceptance. Therefore, we explored whether EVs have biomarker utility in AH as a circulating biomarker. EVs are cell-derived, membrane-defined nanoparticles released by most cell types. Released EVs vary in healthy and diseased states and carry specific cargo signatures that can reflect on the pathophysiologic state of the cell of origin (19, 32, 39, 40). These signatures, along with the relative stability of EVs in circulation, have generated interest in EVs as potential biomarkers (41). In preclinical studies, there is evidence to show that EV production is activated by alcohol administration and that alcohol-induced EVs are key mediators of intercellular and interorgan crosstalk (18, 19, 42). Thus, bioactive EVs are a pathophysiologically-relevant biomarker in AH. Herein, we have demonstrated that total circulating EVs and hepatocyte-derived EVs were significantly elevated in AH and have established a diagnostic cutoff utilizing circulating EV counts. EV counts were significantly higher in AH subjects than heavy drinkers without liver disease, and non-alcohol etiology MELD score matched patients with end-stage liver diseases and alcoholic cirrhosis. Furthermore, the diagnostic performance of EV counts in our complete cohort in differentiating AH from other etiologies of end-stage liver disease was high suggesting that EV counts can serve to diagnose AH in subjects with high MELD scores and ambiguous disease etiology. Thus, following further validation, circulating EVs could serve as a non-invasive, blood-based substitute, also known as liquid biopsy, for liver biopsy [Supplemental Figure 6].

Previously published data from a small, but well-conducted study suggested increased EV counts after binge drinking in healthy subjects (40). In concordance with this study, another important finding of our study was the ability to distinguish heavy drinkers without clinical disease from healthy controls. This suggests a potential role for EVs in identifying relapsed drinking. Thus, if validated, an EV-based biomarker might be used to monitor continued abstinence. This might help identify high-risk patients, especially since new data suggests that heavy drinking, and not mere slips, is associated with increased mortality post-liver transplantation (43).

Even though cutting-edge technology for detecting diverse cellular sources of EVs in circulation is not well developed, we demonstrate a higher abundance of hepatocyte-derived EVs in AH subjects as compared with controls using western-blotting, dual-immunogold labelling, and a novel nPES assay. nPES assay is a technique that utilizes capture antibodies to identify EVs derived from specific cellular sources, in our case CYP2E1 and ASGR2 (36–38). This technique can potentially be translated to a point-of-care test for AH, as it obviates the need to isolate EVs and utilizes 1–5 μL of plasma (36). These data provide insight into the hepatocellular origin of this EV biomarker in AH.

Elegant preclinical studies have shown that alcohol imparts unique cargo to EVs, ceramides are perturbed in AH such that inhibition of ceramide synthesis ameliorates AH in rat models, and ceramides are critical for EV biogenesis (44–48). Combining these observations to develop a pathophysiologically-informed biomarker, we determined selective enrichment of several sphingolipid species in EV cargo in comparison to matched plasma samples. Based on biophysical properties, chylomicrons, LDL, and VLDL are lighter than small EVs isolated at 100,000 *g* and thus float on ultracentrifugation and would not be an expected contaminant (31, 49). For EV sphingolipids, we examined the HDL-specific apoprotein, APOAI, and found comparable expression across controls and AH. Thus, the increase in sphingolipids in AH is not due to a co-isolation of HDL lipoproteins. Furthermore, we do not see an increase in plasma sphingolipids in AH, which would be predominantly bound to lipoprotein particles and albumin. Though we did not expect to isolate VLDL and LDL, we also demonstrate comparable apoprotein, APOB100 across samples. Thus, we demonstrate that our EV isolation and further targeted sphingolipids measurements were free from lipoprotein induced bias. Sphingolipids were found to correlate well with disease severity, by the CTP and MELD scores, and a higher risk for 90-day mortality. Our previous studies have demonstrated that the EV sphingolipid, sphingosine 1-phosphate, plays a key role in macrophage chemotaxis in NASH (50). Many immune cell types and endothelial cells express sphingosine 1-phosphate receptors (50), and indeed, EV-mediated response in these cells may play a role in AH pathogenesis suggesting that these sphingolipid species may be mechanistically relevant to an EV-based biomarker. In addition to increasing the accuracy of EV concentration biomarker, these data also indicate that certain sphingolipid species might be able to define prognosis in AH patients and may be specific targets for AH therapy. Notably, sphingolipid enrichment was not noted in paired plasma samples in our study, in keeping with prior observation of low plasma sphingolipids in malnourished cirrhotics (24). If further validated, these EV biomarkers can be translated to large scale and even automated detection. Novel high throughput technologies, such as nano-scale flow cytometry, nPES, and nano-fluidic devices for EV detection are being developed and may help bring EV-based biomarkers to the clinic.

In the clinical care of AH patients, several clinical models such as MELD, MDF, and Lille score aid in decision-making (10–12). We compared EV counts with MELD scores in subjects with AH and found that EV counts were significantly raised in severe AH (MELD>20) when compared to moderate or mild AH. The prognostic capacity was also determined for EV sphingolipid cargo and was found to be significantly associated with 90-day mortality as well as disease severity. E-MELD, a composite score of MELD, EV count, and specific sphingolipid species together had better discriminatory power than MELD score

alone. This analysis shows the prognostic performance of an EV-based biomarker for predicting severe AH and mortality. Given the ease of repeated blood testing, EVs may permit personalized dynamic risk profiling in AH as resolving AH correlates with a decreasing EV count (16). This concept will need testing in larger longitudinal cohorts.

There are some limitations of this work. Firstly, the sample size is relevant as an exploratory study, and findings need to be validated in larger cohorts. Secondly, not all subjects had liver biopsies. Thirdly, EV cargo analyses were limited to sphingolipids and could have missed changes in other EV cargoes.

In conclusion, we found a circulating EV biomarker to be a promising test to, not only diagnose, but also prognosticate AH. It differentiated AH from other causes of end-stage liver disease including NASH, PBC, and PSC in MELD matched subjects as well as subjects with decompensated alcoholic cirrhosis. EV cargo in AH had a unique sphingolipid signature. These sphingolipids positively correlated with disease severity in AH. They were also associated with increased 90-day mortality. Sphingolipids added to the diagnostic capacity of EV counts and showed promise as a novel predictive model.

Supplementary Material

Refer to Web version on PubMed Central for supplementary material.

ACKNOWLEDGEMENTS

Amy E. Olofson, R.N., for recruiting and consenting subjects for the study. Kayla Gelow, B.S., for her support in collecting TREAT biospecimens and data. Theresa J. Johnson and Courtney Hoover for administrative support. M. Donna Felmlee Devine, M.S., C.C.R.P., for support as clinical coordinator for the Mayo Center for Cell Signaling in Gastroenterology.

Mayo Center for Cell Signaling in Gastroenterology (NIDDK P30DK084567), Translational Research and Evolving Alcoholic Hepatitis Treatment (TREAT) consortium and InTEAM consortium for providing study subject biospecimens.

Mayo Clinic Metabolomics Core (U24DK100469 and UL1TR000135) and Xuan-Mai T. Petterson for sphingolipids measurements.

Financial Support:

NIH-NIAAA grant (U01 AA21788) to H.M. and V.H.S.; NIH-NIAAA grant (R01 AA021171) to V.H.S.; NIH-NIDDK grant (R01 DK11378) to H.M.; ISCIII project PI16/00043 and European Regional Development Fund and Agència de Gestió d'Ajuts Universitaris de Recerca (2017-SGR-01281) to P.G.; and Chile-FONDECYT 1200227 to J.P.A.

Abbreviations

AH	Alcoholic hepatitis
AC	Alcoholic cirrhosis
nPES	nano-plasmonic enhanced scattering assay
ASGR2	Asialoglycoprotein receptor 2
CYP2E1	Cytochrome P450 2E1

NIAAA	National Institute on Alcohol Abuse and Alcoholism
TREAT	Translational Research and Evolving Alcoholic hepatitis Treatment consortium
NTA	Nano-particle tracking analysis
KM	Kaplan-Meier curve
EV	Extracellular vesicles
MELD	Model for end-stage liver disease score
ALD	Alcohol-associated liver disease
NASH	Non-alcoholic steatohepatitis
PBC	Primary biliary cholangitis
PSC	Primary sclerosing cholangitis
ALT	Alanine aminotransferase
AST	Aspartate aminotransferase
ESLD	End-stage liver disease
AUROC curve	Area under the receiver operating characteristic curve
CTP	Child-Turcotte-Pugh score

REFERENCES

1. Griswold MG, Fullman N, Hawley C, Arian N, Zimsen SRM, Tymeson HD, Venkateswaran V, et al. Alcohol use and burden for 195 countries and territories, 1990–2016: a systematic analysis for the Global Burden of Disease Study 2016. The Lancet 2018;392:1015–1035.
2. Paula H, Asrani SK, Boetticher NC, Pedersen R, Shah VH, Kim WR. Alcoholic liver disease-related mortality in the United States: 1980–2003. Am J Gastroenterol 2010;105:1782–1787. [PubMed: 20179691]
3. Szabo G, Kamath PS, Shah VH, Thursz M, Mathurin P. Alcohol-Related Liver Disease: Areas of Consensus, Unmet Needs and Opportunities for Further Study. Hepatology 2019;69:2271–2283. [PubMed: 30645002]
4. Gao B, Bataller R. Alcoholic liver disease: pathogenesis and new therapeutic targets. Gastroenterology 2011;141:1572–1585. [PubMed: 21920463]
5. Sehrawat TS, Liu M, Shah VH. The knowns and unknowns of treatment for alcoholic hepatitis. Lancet Gastroenterology and Hepatology In Press.
6. Seitz HK, Bataller R, Cortez-Pinto H, Gao B, Gual A, Lackner C, Mathurin P, et al. Alcoholic liver disease. Nat Rev Dis Primers 2018;4:16. [PubMed: 30115921]
7. Lucey MR, Mathurin P, Morgan TR. Alcoholic hepatitis. N Engl J Med 2009;360:2758–2769. [PubMed: 19553649]
8. Singal AK, Louvet A, Shah VH, Kamath PS. Grand Rounds: Alcoholic Hepatitis. J Hepatol 2018;69:534–543. [PubMed: 29753761]
9. Dunn W, Jamil LH, Brown LS, Wiesner RH, Kim WR, Menon KV, Malinchoc M, et al. MELD accurately predicts mortality in patients with alcoholic hepatitis. Hepatology 2005;41:353–358. [PubMed: 15660383]

10. Kamath PS, Kim WR. The model for end-stage liver disease (MELD). Hepatology 2007;45:797–805. [PubMed: 17326206]
11. Louvet A, Naveau S, Abdelnour M, Ramond MJ, Diaz E, Fartoux L, Dharancy S, et al. The Lille model: a new tool for therapeutic strategy in patients with severe alcoholic hepatitis treated with steroids. Hepatology 2007;45:1348–1354. [PubMed: 17518367]
12. Maddrey WC, Boitnott JK, Bedine MS, Weber FL Jr., Mezey E, White RI Jr. Corticosteroid therapy of alcoholic hepatitis. Gastroenterology 1978;75:193–199. [PubMed: 352788]
13. Hirsova P, Ibrahim SH, Verma VK, Morton LA, Shah VH, LaRusso NF, Gores GJ, et al. Extracellular vesicles in liver pathobiology: Small particles with big impact. Hepatology 2016;64:2219–2233. [PubMed: 27628960]
14. Lemoinne S, Thabut D, Housset C, Moreau R, Valla D, Boulanger CM, Rautou PE. The emerging roles of microvesicles in liver diseases. Nat Rev Gastroenterol Hepatol 2014;11:350–361. [PubMed: 24492276]
15. Sato K, Meng F, Glaser S, Alpini G. Exosomes in liver pathology. J Hepatol 2016;65:213–221. [PubMed: 26988731]
16. Arab JP, Sehrawat TS, Simonetto DA, Verma VK, Feng D, Tang T, Dreyer K, et al. An Open Label, Dose Escalation Study To Assess The Safety And Efficacy Of IL-22 Agonist F-652 In Patients With Alcoholic Hepatitis. Hepatology;n/a.
17. Thery C, Witwer KW, Aikawa E, Alcaraz MJ, Anderson JD, Andriantsitohaina R, Antoniou A, et al. Minimal information for studies of extracellular vesicles 2018 (MISEV2018): a position statement of the International Society for Extracellular Vesicles and update of the MISEV2014 guidelines. J Extracell Vesicles 2018;7:1535750. [PubMed: 30637094]
18. Verma VK, Li H, Wang R, Hirsova P, Mushref M, Liu Y, Cao S, et al. Alcohol stimulates macrophage activation through caspase-dependent hepatocyte derived release of CD40L containing extracellular vesicles. Journal of Hepatology 2016;64:651–660. [PubMed: 26632633]
19. Bala S, Petrasek J, Mundkur S, Catalano D, Levin I, Ward J, Alao H, et al. Circulating microRNAs in exosomes indicate hepatocyte injury and inflammation in alcoholic, drug-induced, and inflammatory liver diseases. Hepatology 2012;56:1946–1957. [PubMed: 22684891]
20. Iqbal J, Walsh MT, Hammad SM, Cuchel M, Tarugi P, Hegele RA, Davidson NO, et al. Microsomal Triglyceride Transfer Protein Transfers and Determines Plasma Concentrations of Ceramide and Sphingomyelin but Not Glycosylceramide. J Biol Chem 2015;290:25863–25875. [PubMed: 26350457]
21. Lizarazo D, Zabala V, Tong M, Longato L, de la Monte SM. Ceramide inhibitor myriocin restores insulin/insulin growth factor signaling for liver remodeling in experimental alcohol-related steatohepatitis. Journal of Gastroenterology and Hepatology 2013;28:1660–1668. [PubMed: 23802886]
22. Longato L, Ripp K, Setshedi M, Dostalek M, Akhlaghi F, Branda M, Wands JR, et al. Insulin Resistance, Ceramide Accumulation, and Endoplasmic Reticulum Stress in Human Chronic Alcohol-Related Liver Disease. Oxidative Medicine and Cellular Longevity 2012;2012:17.
23. Rachakonda V, Gabbert C, Raina A, Bell LN, Cooper S, Malik S, Behari J. Serum Metabolomic Profiling in Acute Alcoholic Hepatitis Identifies Multiple Dysregulated Pathways. PLOS ONE 2014;9:e113860. [PubMed: 25461442]
24. Rachakonda V, Argemi J, Borhani AA, Bataller R, Tevar A, Behari J. Reduced Serum Sphingolipids Constitute a Molecular Signature of Malnutrition in Hospitalized Patients With Decompensated Cirrhosis. Clin Transl Gastroenterol 2019;10:e00013. [PubMed: 30908309]
25. Liangpunsakul S, Sozio MS, Shin E, Zhao Z, Xu Y, Ross RA, Zeng Y, et al. Inhibitory effect of ethanol on AMPK phosphorylation is mediated in part through elevated ceramide levels. Am J Physiol Gastrointest Liver Physiol 2010;298:G1004–1012. [PubMed: 20224005]
26. Supakul R, Liangpunsakul S. Alcoholic-induced hepatic steatosis--role of ceramide and protein phosphatase 2A. Transl Res 2011;158:77–81. [PubMed: 21757150]
27. Peeraphatdit TB, Kamath PS, Karpyak VM, Davis B, Desai V, Liangpunsakul S, Sanyal A, et al. Alcohol Rehabilitation Within 30 Days of Hospital Discharge Is Associated With Reduced Readmission, Relapse, and Death in Patients With Alcoholic Hepatitis. Clin Gastroenterol Hepatol 2019.

28. Crabb DW, Bataller R, Chalasani NP, Kamath PS, Lucey M, Mathurin P, McClain C, et al. Standard Definitions and Common Data Elements for Clinical Trials in Patients With Alcoholic Hepatitis: Recommendation From the NIAAA Alcoholic Hepatitis Consortia. Gastroenterology 2016;150:785–790. [PubMed: 26921783]
29. Singal AK, Bataller R, Ahn J, Kamath PS, Shah VH. ACG Clinical Guideline: Alcoholic Liver Disease. Am J Gastroenterol 2018;113:175–194. [PubMed: 29336434]
30. Eguchi A, Lazaro RG, Wang J, Kim J, Povero D, Willliams B, Ho SB, et al. Extracellular vesicles released by hepatocytes from gastric infusion model of alcoholic liver disease contain a MicroRNA barcode that can be detected in blood. Hepatology 2017;65:475–490. [PubMed: 27639178]
31. Mathieu M, Martin-Jaular L, Lavieu G, Théry C. Specificities of secretion and uptake of exosomes and other extracellular vesicles for cell-to-cell communication. Nature Cell Biology 2019;21:9–17. [PubMed: 30602770]
32. Povero D, Eguchi A, Li H, Johnson CD, Papouchado BG, Wree A, Messer K, et al. Circulating extracellular vesicles with specific proteome and liver microRNAs are potential biomarkers for liver injury in experimental fatty liver disease. PLoS One 2014;9:e113651. [PubMed: 25470250]
33. Severino V, Dumonceau JM, Delhaye M, Moll S, Annessi-Ramseyer I, Robin X, Frossard JL, et al. Extracellular Vesicles in Bile as Markers of Malignant Biliary Stenoses. Gastroenterology 2017;153:495–504.e498. [PubMed: 28479376]
34. Théry C, Amigorena S, Raposo G, Clayton A. Isolation and Characterization of Exosomes from Cell Culture Supernatants and Biological Fluids. Current Protocols in Cell Biology 2006;30:3.22.21–23.22.29.
35. Crabb DW, Im GY, Szabo G, Mellinger JL, Lucey MR. Diagnosis and Treatment of Alcohol-Related Liver Diseases: 2019 Practice Guidance from the American Association for the Study of Liver Diseases. Hepatology 2019.
36. Liang K, Liu F, Fan J, Sun D, Liu C, Lyon CJ, Bernard DW, et al. Nanoplasmonic Quantification of Tumor-derived Extracellular Vesicles in Plasma Microsamples for Diagnosis and Treatment Monitoring. Nat Biomed Eng 2017;1.
37. D'Souza AA, Devarajan PV. Asialoglycoprotein receptor mediated hepatocyte targeting - strategies and applications. J Control Release 2015;203:126–139. [PubMed: 25701309]
38. Wu D, Cederbaum AI. Presence of functionally active cytochrome P-450IIE1 in the plasma membrane of rat hepatocytes. Hepatology 1992;15:515–524. [PubMed: 1544634]
39. Fukushima M, Dasgupta D, Mauer AS, Kakazu E, Nakao K, Malhi H. StAR-related lipid transfer domain 11 (STARD11)-mediated ceramide transport mediates extracellular vesicle biogenesis. J Biol Chem 2018;293:15277–15289. [PubMed: 30139741]
40. Momen-Heravi F, Bala S, Kodys K, Szabo G. Exosomes derived from alcohol-treated hepatocytes horizontally transfer liver specific miRNA-122 and sensitize monocytes to LPS. Sci Rep 2015;5:9991. [PubMed: 25973575]
41. Théry C, Zitvogel L, Amigorena S. Exosomes: composition, biogenesis and function. Nature Reviews Immunology 2002;2:569–579.
42. Eguchi A, Kostallari E, Feldstein AE, Shah VH. Extracellular vesicles, the liquid biopsy of the future. J Hepatol 2019;70:1292–1294. [PubMed: 30982591]
43. Lee BP, Mehta N, Platt L, Gurakar A, Rice JP, Lucey MR, Im GY, et al. Outcomes of Early Liver Transplantation for Patients With Severe Alcoholic Hepatitis. Gastroenterology 2018;155:422–430.e421. [PubMed: 29655837]
44. Choi S, Snider AJ. Sphingolipids in High Fat Diet and Obesity-Related Diseases. Mediators Inflamm 2015;2015:520618. [PubMed: 26648664]
45. Maceyka M, Spiegel S. Sphingolipid metabolites in inflammatory disease. Nature 2014;510:58–67. [PubMed: 24899305]
46. Mauer AS, Hirsova P, Maiers JL, Shah VH, Malhi H. Inhibition of sphingosine 1-phosphate signaling ameliorates murine nonalcoholic steatohepatitis. Am J Physiol Gastrointest Liver Physiol 2017;312:G300–g313. [PubMed: 28039158]

47. Nojima H, Freeman CM, Schuster RM, Japtok L, Kleuser B, Edwards MJ, Gulbins E, et al. Hepatocyte exosomes mediate liver repair and regeneration via sphingosine-1-phosphate. Journal of Hepatology 2016;64:60–68. [PubMed: 26254847]

48. Trajkovic K, Hsu C, Chiantia S, Rajendran L, Wenzel D, Wieland F, Schwille P, et al. Ceramide Triggers Budding of Exosome Vesicles into Multivesicular Endosomes. Science 2008;319:1244–1247. [PubMed: 18309083]

49. Simonsen JB. What Are We Looking At? Extracellular Vesicles, Lipoproteins, or Both? Circulation Research 2017;121:920–922. [PubMed: 28963190]

50. Liao CY, Song MJ, Gao Y, Mauer AS, Revzin A, Malhi H. Hepatocyte-Derived Lipotoxic Extracellular Vesicle Sphingosine 1-Phosphate Induces Macrophage Chemotaxis. Front Immunol 2018;9:2980. [PubMed: 30619336]

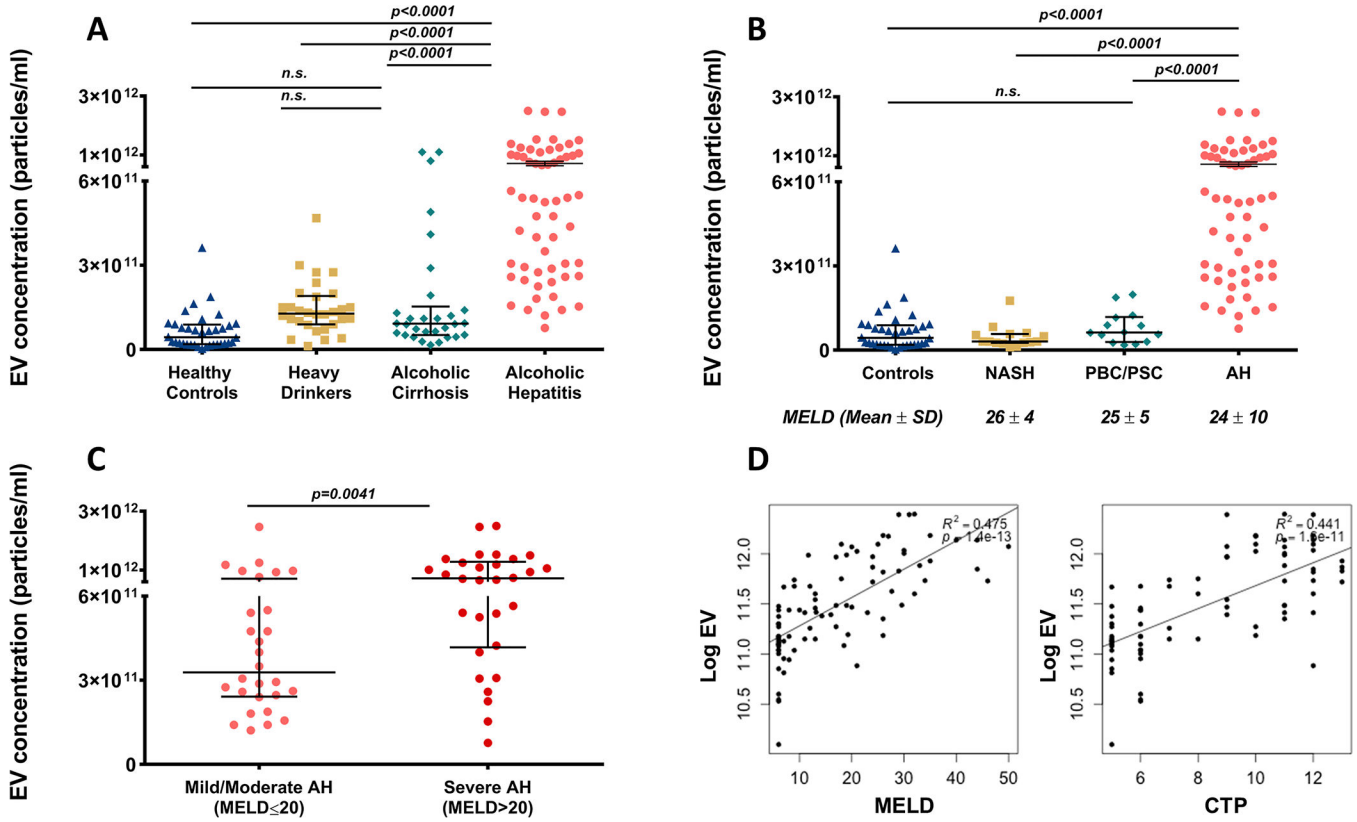

Figure 1: EVs are elevated in plasma from AH subjects and correlate with disease severity.

(A) EV counts were significantly elevated in AH when compared to healthy controls ($p<0.0001$), heavy drinkers ($p<0.0001$), and decompensated alcoholic cirrhosis subjects ($p<0.0001$). Heavy drinkers had significantly higher EV counts than healthy controls ($p=0.0068$). (B) EV counts were significantly higher in AH when compared to ESLD ($p<0.0001$). MELD scores were comparable between NASH, cholestatic liver diseases, and AH subgroups. (C) EV counts were significantly higher in severe AH subjects (MELD>20) when compared with mild/moderate AH subjects. (D) EV counts were also significantly correlated with MELD and CTP scores ($p<0.0001$).

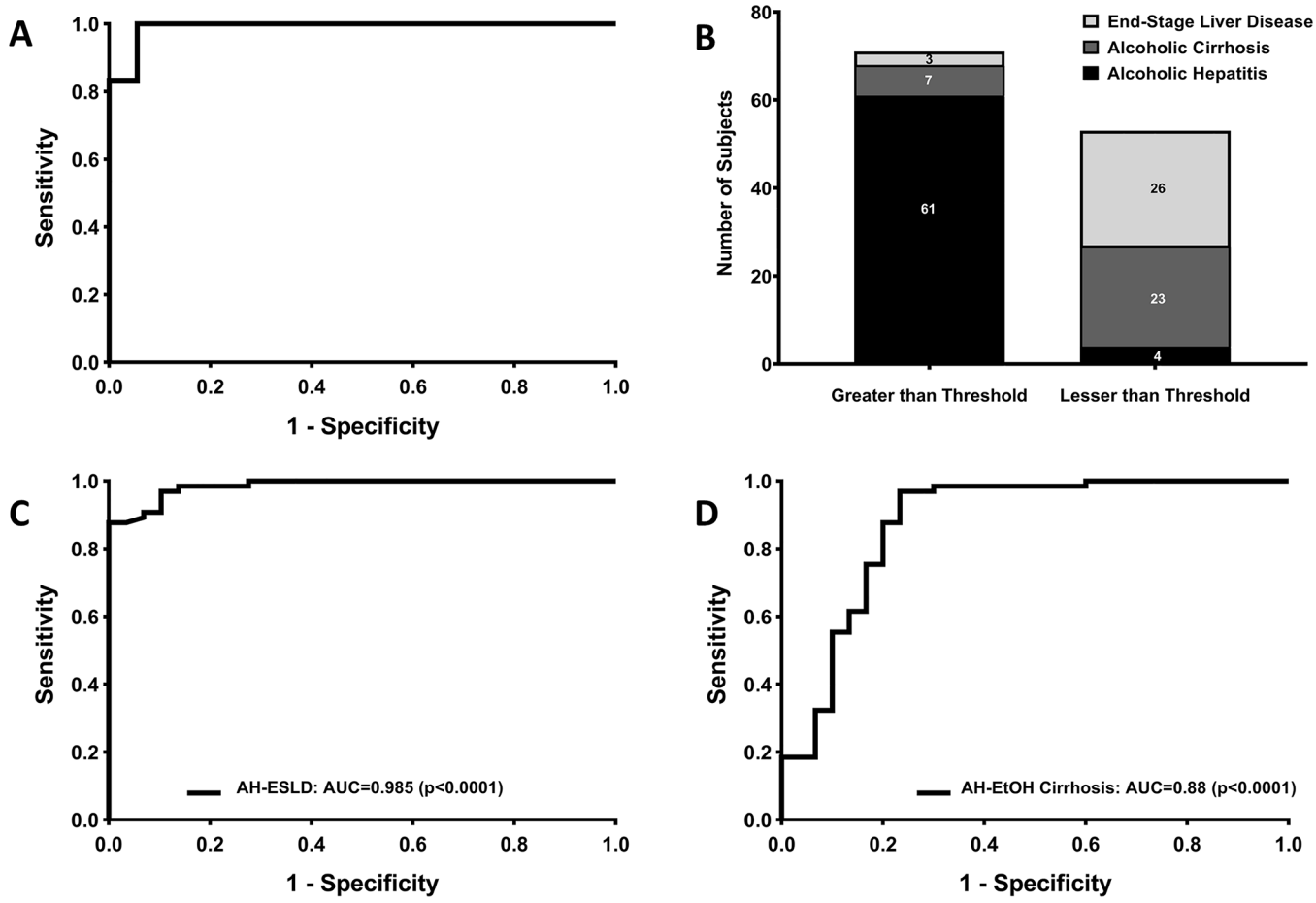

Figure 2: EV concentration has high performance in diagnosing AH.

(A) High diagnostic accuracy was noted for diagnosis of AH versus healthy controls in the discovery cohort. A cut-off value of 1.56×10^{11} particles/ml was determined using Youden's index. **(B)** In the complete cohort, using 1.56×10^{11} particles/ml, we were able to diagnose AH vs. MELD matched severe end-stage liver disease and decompensated alcoholic cirrhosis subjects with high sensitivity and specificity. **(C)** The diagnostic performance in our complete cohort of AH subjects was high compared to MELD-matched severe end-stage liver disease subjects with NASH or cholestatic liver diseases. **(D)** The diagnostic performance in our complete cohort of AH subjects was high compared to decompensated alcoholic cirrhosis subjects.

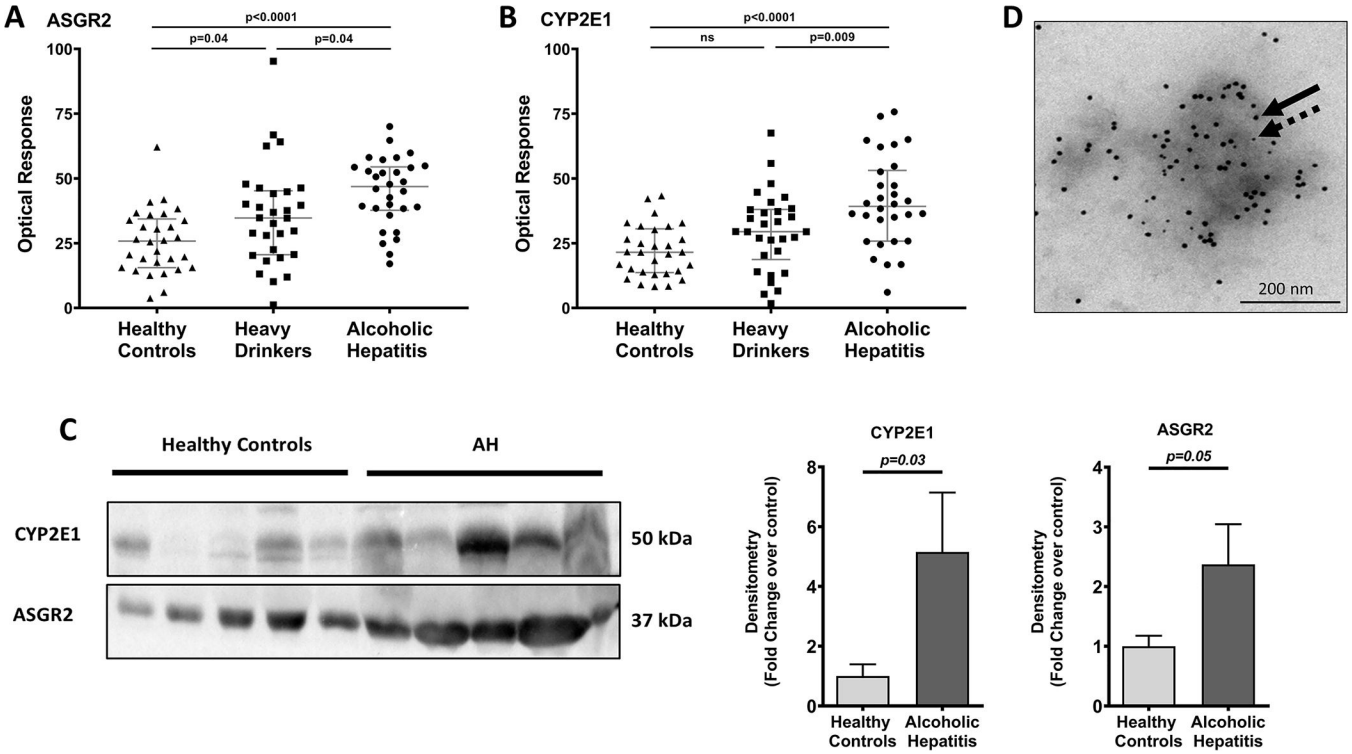

Figure 3: Hepatocyte-derived EVs are increased in AH subjects.

(A) Optical response with ASGR2 antibody is higher in AH subjects than in healthy controls ($p<0.0001$) and heavy drinkers ($p<0.0001$). (n=30 for all groups) **(B)** Optical response with CYP2E1 antibody is higher in AH subjects than in healthy controls ($p<0.0001$) and heavy drinkers ($p<0.0001$). (n=30 for all groups) **(C)** Immunoblotting was performed for hepatocyte-specific markers CYP2E1 and ASGR2 and revealed an increased number of hepatocyte derived EVs in AH (n=3 for all groups). EVs used for each sample were isolated from identical volumes of plasma. **(D)** Representative transmission electron micrograph of isolated plasma EVs from an AH subject. Dual immunogold labeling was performed for two hepatocyte specific markers, CYP2E1 and ASGR2. The larger beads (15nm, labelled as solid arrow) detect ASGR2 and the smaller beads (10 nm, labelled as dashed arrow) detect CYP2E1. There was high abundance of hepatocyte specific proteins in the isolated EVs from AH subjects' plasma.

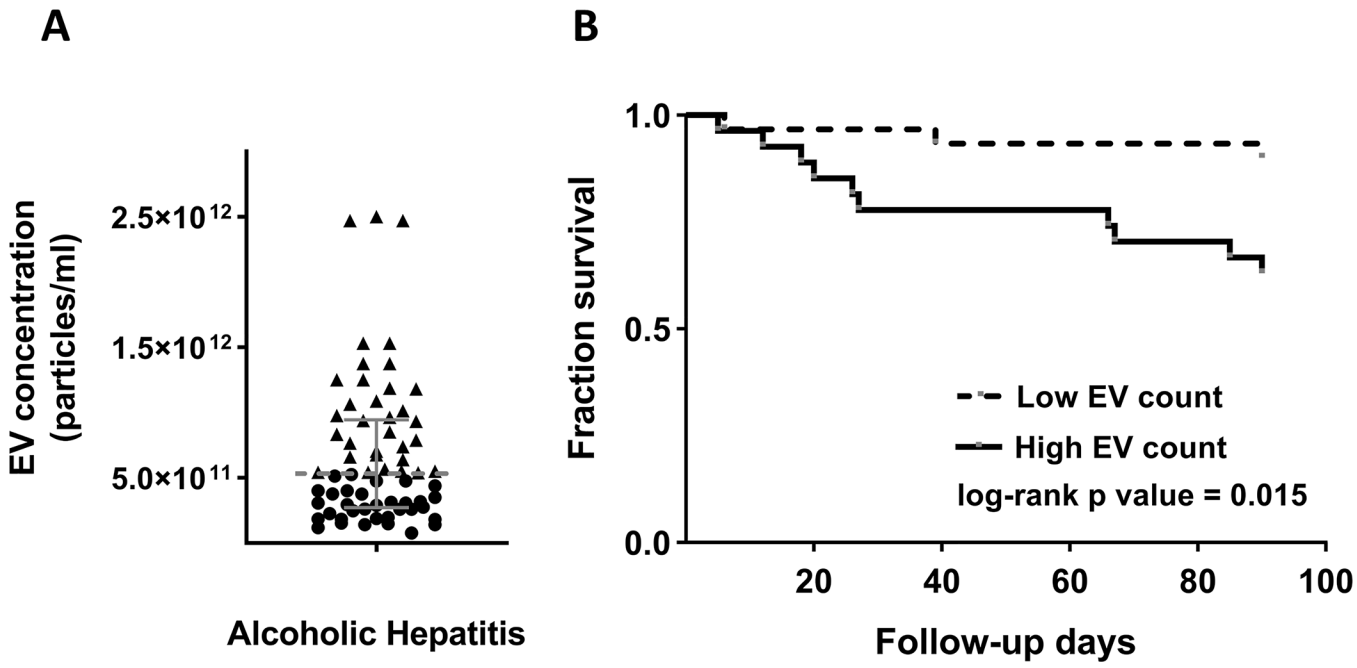

Figure 4: EV counts have utility in predicting 90-day survival.

(A) AH subjects were dichotomized at the median and divided into two subgroups of high and low EV counts. **(B)** Patients in the high EV count group had significantly higher 90-day mortality compared to patients in the low EV count group (logrank p=0.015).

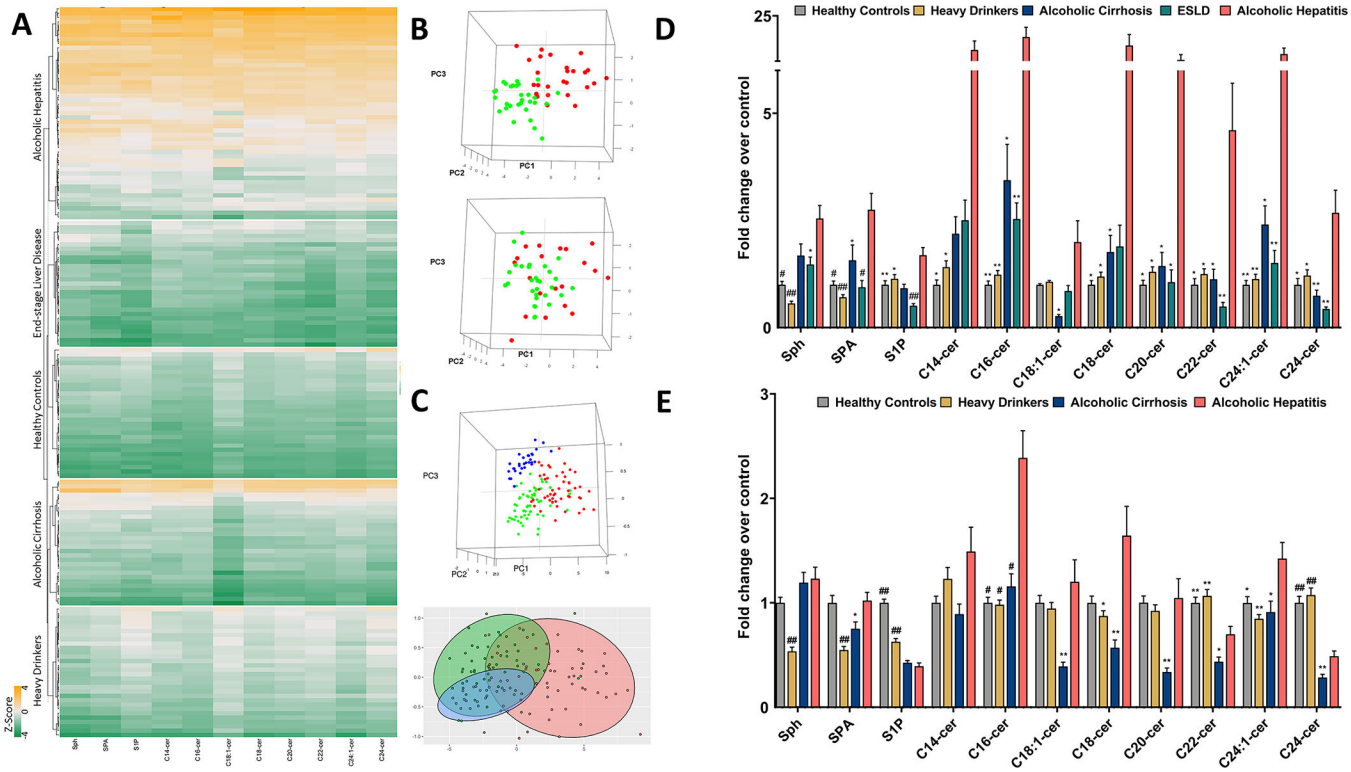

Figure 5: EV cargo is enriched in sphingolipid species in AH subjects.

(A) Heatmap and hierarchical clustering depicts differences in concentration of sphingolipid species in healthy controls, heavy drinkers, alcoholic cirrhosis, ESLD, and alcoholic hepatitis subjects. EV sphingolipid cargo from healthy controls and ESLD subjects clusters together and cargo from alcoholic cirrhosis and heavy drinkers cluster together. EVs from AH subjects are highly-enriched in multiple sphingolipid species and cluster separately. **(B)** 3D principal component analysis (PCA) graphs demonstrate differential clustering of sphingolipid species in EVs and plasma from healthy controls (green) and AH subjects (red). **(C)** 3D and 2D PCA graphs help demonstrate differential clustering of sphingolipid species in EV cargo from healthy controls (green), cirrhotics including alcoholic, NASH, PBC, and PSC subjects (blue), and AH subjects (red). **(D)** Multiple sphingolipid species, especially long chain ceramides, were significantly raised in AH compared with healthy controls, heavy drinkers, decompensated AC and ESLD subjects. These values are shown here as fold-change over controls. **(E)** In contrast, only C16:0 ceramide and C24:1 ceramide showed significantly increased concentration in AH. p-values of ≤0.05, 0.01, 0.001, and 0.0001 were denoted as *, **, #, and ## respectively.

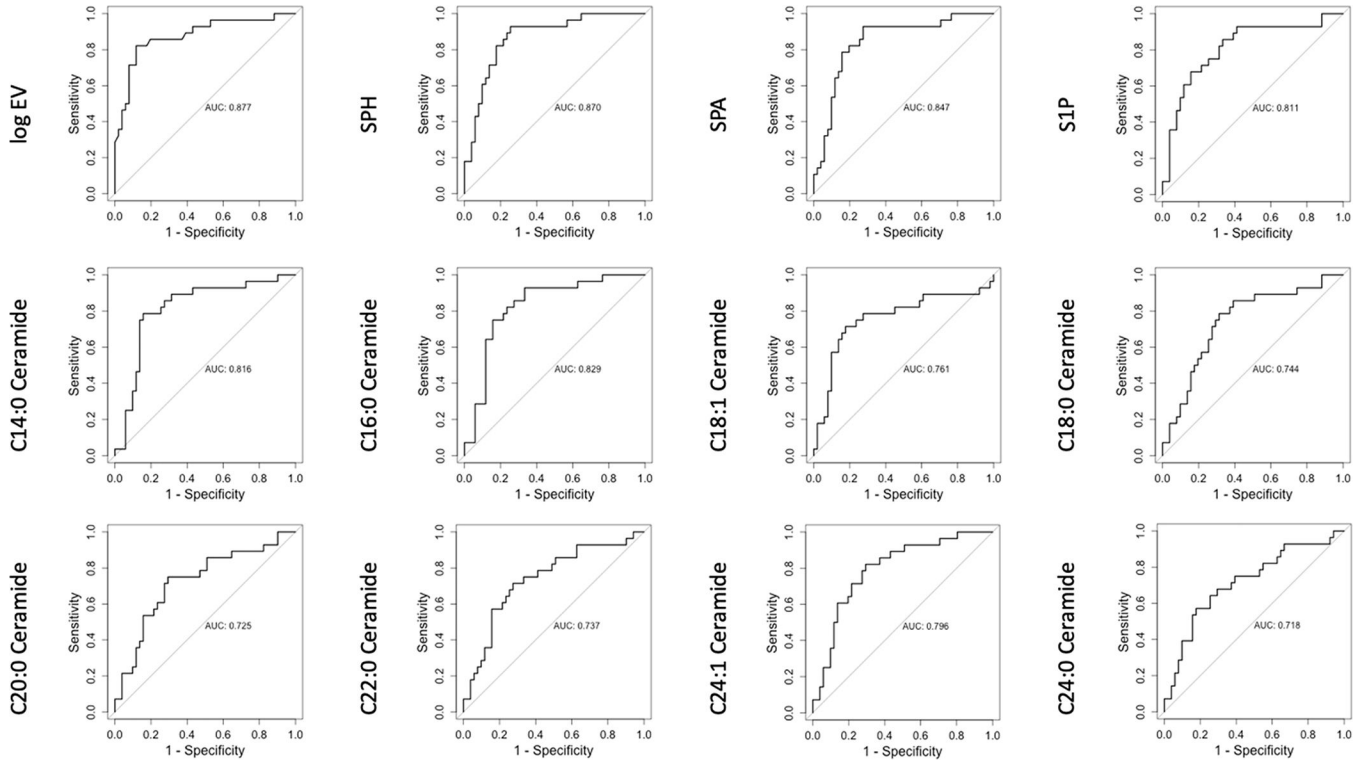

Figure 6: EV sphingolipid cargo can predict severity of disease in AH subjects.

ROC curves were generated to assess role of EV and individual sphingolipids in predicting disease severity. Log EV (AUC=0.88, p=<0.0001), SPH (AUC=0.85, p<0.0001), SPA (AUC=0.85, p<0.0001), S1P (AUC=0.81, p=0.0002), C14:0 ceramide (AUC=0.82, p=0.0001), C16:0 ceramide (AUC=0.83, p<0.0001), C18:1 ceramide (AUC=0.76, p=0.0009), C18:0 ceramide (AUC=0.74, p=0.001), C20:0 ceramide (AUC=0.73, p=0.001), C22:0 ceramide (AUC=0.74, p=0.001), C24:1 ceramide (AUC=0.80, 0.0001), and C24:0 (AUC=0.72, 0.002) all resulted in significant ROC curves with high AUROC curve values. (SPH=sphingosine, SPA=sphinganine, and S1P=Sphingosine 1-phosphate).

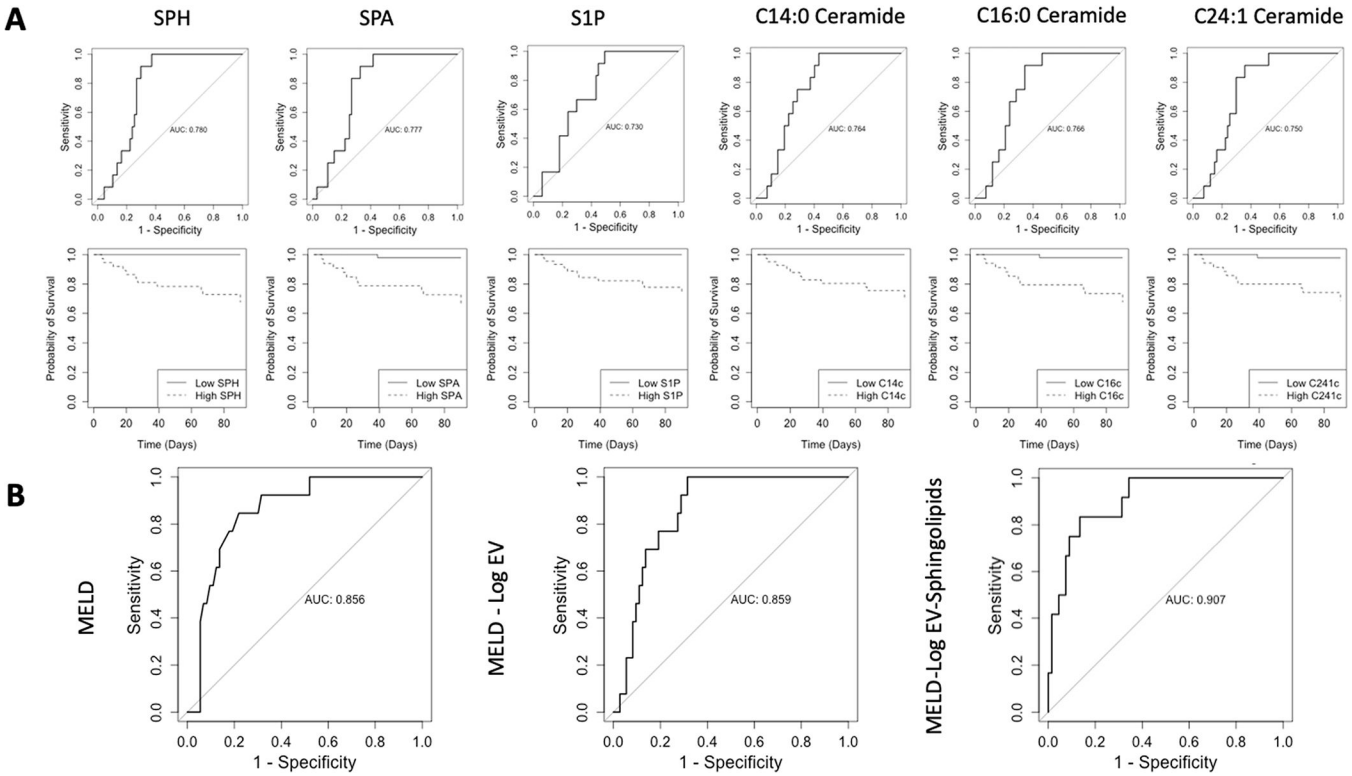

Figure 7: EV sphingolipid may improve the performance of MELD score.

(A) ROC curves were generated to assess the role of EV and individual sphingolipids in predicting 90-day mortality in subjects. Again, the same sphingolipid species had the best performance. Log EV (AUC=0.81, p=0.003), SPH (AUC=0.78, p=0.008), SPA (AUC=0.78, p=0.009), S1P (AUC=0.73, p=0.04), C14:0 ceramide (AUC=0.76, p=0.03), C16:0 ceramide (AUC=0.77, p=0.01), and C24:1 ceramide (AUC=0.75, p=0.03) all resulted in statistically-significant ROC curves. Youden's index was used to assess optimal cut-off to dichotomize the cohort for predicting 90-day mortality, and these were then used to generate KM curves for predicting survival. All 6 EV × sphingolipid species resulted in statistically-significant KM curve graphs (all $p<0.01$). **(B)** Log EV count and sphingolipid cargo improved the performance of MELD score in predicting 90-day mortality in our cohort. MELD had an AUC value of 0.86. When log EV was taken into consideration with MELD, the AUC did not improve. However, on addition of the 6 sphingolipid species, which were found to be significantly associated with 90-day mortality in Cox's univariate analysis to MELD and logEV, the AUC value increased to 0.91. (SPH=sphingosine, SPA=sphinganine, and S1P=Sphingosine 1-phosphate).

TABLE 1.

Circulating EV Counts

EV concentration (particles/ml)	Healthy Controls	Heavy Drinkers	NASH	PBC and PSC	Decompensated Alcoholic Cirrhosis	Alcoholic Hepatitis
Minimum	2.8×10^{9}	1.25×10^{10}	1.08×10^{10}	1.8×10^{10}	1.6×10^{10}	7.65×10^{10}
25^{th} Percentile	1.91×10^{10}	8.94×10^{10}	2.6×10^{10}	2.9×10^{10}	5.18×10^{10}	2.75×10^{11}
Median	4.38×10^{10}	1.28×10^{11}	3.06×10^{10}	6.29×10^{10}	9.2×10^{10}	5.38×10^{11}
75^{th} Percentile	8.88×10^{10}	1.91×10^{11}	5.74×10^{10}	1.18×10^{11}	1.53×10^{11}	1.01×10^{12}
Maximum	3.63×10^{11}	4.68×10^{11}	1.76×10^{11}	1.98×10^{11}	1.1×10^{12}	2.5×10^{12}

Statistical comparisons of EV counts: AH vs. healthy controls ($p<0.0001$), AH vs. heavy drinkers ($p=0.0001$), AH vs. NASH and cholestatic liver diseases ($p<0.0001$), AH vs. decompensated alcoholic cirrhosis ($p<0.0001$).